Mobile Terminal Energy Management for Sustainable Multi-homing Video Transmission

Muhammad Ismail, *Member, IEEE,* and Weihua Zhuang, *Fellow, IEEE*

***Abstract*—In this paper, an energy management sub-system is proposed for mobile terminals (MTs) to support a sustainable multi-homing video transmission, over the call duration, in a heterogeneous wireless access medium. Through statistical video quality guarantee, the MT can determine a target video quality lower bound that can be supported for a target call duration. The target video quality lower bound captures the MT available energy at the beginning of the call, the time varying bandwidth availability and channel conditions at different radio interfaces, the target call duration, and the video packet characteristics in terms of distortion impact, delay deadlines, and video packet encoding statistics. The MT then adapts its energy consumption to support at least the target video quality lower bound during the call. Simulation results demonstrate the superior performance of the proposed framework over two benchmarks, and some performance trade-offs.**

***Index Terms*—Mobile terminal energy management, multi-homing video transmission, video packet scheduling, statistical performance guarantees, heterogeneous wireless access medium, precedence-constrained multiple knapsack problem (PC-MKP).**

I. Introduction

The wireless communication medium has become a heterogeneous environment with various wireless access options and overlapped coverage from different networks. As a result, currently there exists a variety of opportunities for mobile users to enhance their transmission/reception data rate and hence improve the perceived quality-of-service (QoS). Mobile terminals (MTs) are now equipped with multiple radio interfaces in order to take advantage of these available opportunities. One promising service in this networking environment is referred to as a multi-homing service, where an MT utilizes all its radio interfaces simultaneously to aggregate the offered resources from different networks in order to support the same application [2] - [4].

Recently, video streaming has gained an increasing popularity among mobile services. It has been reported that 65% of all mobile data traffic, by the end of 2015, will be due to mobile video traffic [5]. Multi-homing video transmission can benefit the achieved video quality in many aspects [6], [7]. Firstly, sending video packets over multiple networks increases the amount of aggregate bandwidth available to the application and hence increases the quality of the delivered service. Secondly, sending video packets over multiple networks can reduce the correlation between consecutive packet losses due to transmission errors or networks' congestion. Finally, video packet transmission over multiple networks allows for better mobility support which significantly reduces the probability of an outage when communication is lost with the current serving network due to user mobility out of its coverage area.

Recent studies have shown that the gap between the demand for energy and the offered MT battery capacity is increasing exponentially with time [8]. As a result, the MT operational time in between battery charging has become a significant factor in the user perceived QoS [9]. In addition to developing new battery technology with improved capacity, the MT operational period between battery charging can be extended through effective management of its energy consumption [10].

Consider an uplink multi-homing video transmission from an MT [5]. In the absence of an appropriate energy management strategy, the MT can use up all its available energy and hence drain its battery before call completion. As a result, an energy management strategy is required in order to ensure a sustainable video transmission, over different radio interfaces, for the call duration. However, this problem has been overlooked, so far, in literature. A simple energy management sub-system can equally distribute the MT available energy over different time slots of the video call duration. Given the time varying bandwidth availability and channel conditions over different time slots, using this uniform energy distribution will lead to inconsistent temporal fluctuations in the video quality. An appropriate energy management sub-system should use the MT energy in a way such that it can support a consistent video quality in the call duration over time varying bandwidth availability and channel conditions.

In this paper, an energy management sub-system is proposed for MTs to support a sustainable multi-homing video transmission in a fading channel, over a target call duration, in a heterogeneous wireless access medium. The contributions of this paper are summarized in the following:

- A two-stage energy management sub-system is proposed. In the first stage, through video quality statistical guarantee, the MT can determine a target video quality lower bound that can be supported for a target call duration with a small outage probability. In the second stage, the MT adapts its energy consumption during the call, following a three-step framework, to achieve at least the target video quality lower bound;
- We develop an efficient framework to provide QoS statistical guarantee for multi-homing video transmission while considering the video packet characteristics. Using this framework, we provide an expression for the cumulative distribution function (CDF) of the video quality that can

The authors are with the Department of Electrical and Computer Engineering, University of Waterloo, Waterloo, Canada, e-mail:{m6ismail, wzhuang}@uwaterloo.ca.

This paper will be presented in part at IEEE Globecom 2013 [1].

be achieved in a multi-homing scenario, given the MT available energy at the beginning of the call, the time varying bandwidth availability and channel condition at different radio interfaces, the target call duration, and the video packet characteristics in terms of distortion impact, delay deadlines, and packet encoding statistics. The video quality CDF is then used to derive the maximum video quality lower bound that can be supported for the target call duration;

- We develop a three-step framework that can adapt the MT energy consumption, during the call, to satisfy at least the target video quality lower bound calculated in the call set-up. The framework determines the minimum required power allocation for the radio interfaces to satisfy the target video quality lower bound, selectively drops some packets given the allocated power at different radio interfaces, and assigns remaining packets to different radio interfaces;
- We compare the proposed energy management sub-system to two benchmarks to evaluate its performance. Through computer simulations, we show that the proposed energy management sub-system guarantees a sustainable multi-homing video transmission over the call duration with a consistent video quality as compared to the benchmarks. In addition, we investigate some performance trade-offs for the proposed energy management sub-system.

The rest of this paper is organized as follows: In Section II, the related work is reviewed. The system model is presented in Section III. The energy management sub-system for sustainable multi-homing video transmission is developed in Section IV. Simulation results are presented in Section VII. Finally, conclusions are given in Section VIII. Table I summarizes the important mathematical symbols.

TABLE I: Summary of Important Symbols

Symbol	Definition
$\mathcal{A}_k^f$	Set of ancestors for packet k of frame f
b_n	Allocated bandwidth on the uplink to the MT nth radio interface
c_f	Number of video packets for frame f
d_f	Delay deadline of a packet that belongs to frame f
E	MT available Energy at the beginning of the call
E_t	MT available energy at beginning of time slot t
$\mathcal{F}$	Set of available video frames
$\mathcal{S}_n$	Set of assigned packets to the nth radio interface
$\mathcal{S}$	Set of assigned packets to all radio interfaces
l_f	Length in bits for a packet of frame f
$\mathcal{N}$	Set of utilized radio interfaces
P_n	Instantaneous allocated power to the nth radio interface
$\bar{P}_n$	Average allocated power to the nth radio interface
q_t	Video quality value for time slot t
q_l	Target video quality lower bound
r_{n,m_n}	Data rate that can be supported at the nth radio interface
$r(k_f)$	Required minimum data rate for transmitting packet k of frame f
r	Total required data rate to support at least the video quality lower bound q_l
T	Total number of time slots for the target call duration
T_c	Video call duration
v_f	Distortion impact of a packet that belongs to frame f
x_{kn}^f	Binary decision variable for assignment of packet k of frame f to radio interface n
τ	Time slot duration
ϵ_q	Outage probability for supporting video quality at least equals to q_l
ϵ_c	Outage probability for supporting the entire call duration
γ_n	Received SNR at the BS/AP communicating with the nth radio interface at a given time slot
$\bar{\gamma}_n$	Average received SNR at the BS/AP communicating with the nth radio interface
Γ_{n,m_n}	Received SNR threshold to support data rate r_{n,m_n} at radio interface n
Ω_n	Average channel power gain for radio interface n
η_0	Noise power spectral density
$\Delta D_{f+1,f}$	Difference in delay deadline for two consecutive frames

II. Related Work

In literature, there are several studies on how to achieve high video quality with low power consumption. In these works, the main objective is to design energy efficient video packet scheduling mechanisms. Two categories of video packet scheduling mechanisms can be distinguished. The first category includes single-path video transmission techniques, while the second category includes video transmission over multiple network paths.

In single-path video transmission, the main objective is to schedule video packet transmission so that packets do not miss their playback deadline. Video packets whose playback deadlines have passed are dropped in order not to waste network resources. The scheduling policy should capture video packet characteristics in terms of delay deadlines and distortion impacts, and the time varying wireless channel conditions. In [11] and [12], the video packet scheduling problem is formulated as a Markov decision process (MDP) that balances the achieved video quality and the consumed energy. One limitation of extending an MDP formulation to a multi-homing scenario is the curse of dimensionality as the state space and actions will suffer from an exponential growth as a function of the number of the available networks. Energy budget is considered in the video packet scheduling framework of [13]. The work of [5] addresses the problem of joint packet scheduling and power allocation in order to minimize video quality distortion.

Various works in literature have investigated packet scheduling for multi-path video streaming. In [14], the video streaming policy consists of a joint selection of the network path and the video packets to be transmitted, along with their sending times. While [15] and [16] deal with multi-path video transmission over wireless links, no attention is given to the transmission power allocation and the associated energy constraints. For mobile ad hoc networks, when energy efficiency is discussed, as in [17] and [18], the objective is to schedule packets on paths with sufficient energy and avoid paths where nodes are suffering from energy depletion. The work of [19] studies video transmission in a heterogeneous wireless access medium and employs multi-homing service in downlink transmission, hence it does not deal with MT energy consumption. Energy efficient multi-homing schedulers are proposed in [20] and [21], however, again for downlink transmission.

Minimizing energy consumption (e.g., [11]) does not guarantee that the MT available energy can support video transmission over the call duration, given the battery energy limitation. In addition, related works deal with an energy budget per time slot (e.g., [13] and [22]) in the presence of an energy management sub-system which can determine the energy budget per time slot to ensure a sustainable video transmission over the call duration. However, not many details are given regarding this energy management sub-system. A simple energy management sub-system can equally distribute the MT available energy over different time slots. Given the time varying video packet encoding, bandwidth availability, and channel conditions at different radio interfaces, using this uniform energy distribution will lead to inconsistent temporal fluctuations in the video quality. Instead, an appropriate energy management sub-system should use the MT energy in a way such that it can support the call duration with a consistent video quality over time slots, independent of varying packet encoding, bandwidth availability, and channel conditions.

None of the existing works in literature provides a statistical guarantee for multi-homing video transmission to complete the call with a consistent quality. In literature, one approach to provide performance statistical guarantee is through the effective bandwidth and effective capacity concepts, as in [23]. However, the work in [23] mainly addresses single-network video transmission and does not provide an energy efficient design. Adopting the effective bandwidth and effective capacity concepts in providing performance statistical guarantees imposes some restrictions on the service process, in order to develop an effective capacity expression that is easy to compute and to handle. Hence, the problem formulation would not incorporate many details (i.e., MT available energy at the beginning of the call, the call duration, radio interface characteristics in terms of time varying offered bandwidth and channel conditions, and video packet characteristics in terms of distortion impact, delay deadline, and packet encoding).

III. System Model

A. Video Packet-level Traffic Model

The video sequence is encoded into a bit stream using a layered/scalable video encoder. The layered representation of the video sequence is composed of a base layer and several enhancement layers [24]. The base layer, which can be decoded independently of the enhancement layers, provides a basic level of video quality. The decoding of enhancement layers is based on the base layer and serves to improve the base layer quality. Each video layer is periodically encoded using a group-of-picture (GoP) structure. Time is partitioned into time slots, $\mathcal{T} = \{1, 2, \ldots, T\}$, of equal duration τ, where $T = \lceil \frac{T_c}{\tau} \rceil$ and T_c denotes the call duration. Since the call duration, T_c, is a random variable, as will be explained in the next subsection, T is also a random variable. Every time slot, the MT has a new GoP, from different layers, ready for transmission. Hence, the time slot duration is determined based on the source encoding rate in frames per second (fps). Each time slot has $\mathcal{F}$ frames from different layers, $\mathcal{F} = \{1, 2, \ldots, F\}$, and each frame can be of I, P, or B type. I Frames are compressed versions of raw frames independent of other frames. P frames only refer to preceding I/P frames, while B frames can refer to both preceding and succeeding frames. The data within one time slot are encoded inter-dependently through motion estimation, while data belonging to different time slots are encoded independently [11]. A video frame has the following characteristics [11]:

- Size - Each frame f is encoded into packets and each packet contains data relative to at most one frame [14]. Frame f is fragmented into C_f packets, $C_f \in [1, C_{f,\max}]$, where $C_{f,\max}$ denotes the maximum allowable size for frame f at each GoP. The frame size (in numbers of video packets, C_f) is represented by an independent identically distributed (i.i.d.) random variable that follows a probability mass function (PMF) $f_{C_f}(c_f)$ [11]. The frame size across different GoPs follows the same PMF given the frame type (I, P, or B). The PMF, $f_{C_f}(c_f)$, can be calculated for different video contents and frame types as in [25]. The frame size, C_f, for frames of I, P, or B types is constant within one time slot[1] and varies from one time slot to another. The packet size (in bits) for frame f is denoted by l_f.
- Distortion Impact - Each frame, f, has a distortion impact value per packet, v_f[2]. It represents the amount by which video distortion is reduced if this packet is received, on time, at the decoder side. The packet distortion impact value, v_f, for different video contents and frame types can be calculated as discussed in [26].
- Delay Deadline - It represents the time by which the frame should be decoded at the destination, which is also known as decoding time stamp [5]. Packets that belong to the same frame have the same delay deadline, which is denoted by d_f. Since videos are encoded using a fixed number of fps within the same layer, the difference in the delay deadline between any two consecutive frames within the layer is constant [5]. The delay difference is given by $|d_{f+1} - d_f| = \Delta D_{f+1,f}$. The transmission deadlines of all packets within a given GoP expire within τ.
- Dependence - Within each time slot, since some frames are encoded based on the prediction of other frames, there are dependencies among these frames. Hence, packet decoding of one frame depends on the successful decoding of packets from other frames. These dependencies among packets of different frames, within one time slot, are expressed using a directed acyclic graph (DAG) [11], as shown in Figure 1. Hence, each video packet k_f is said to have ancestors $\mathcal{A}_k^f$. Packets which belong to $\mathcal{A}_k^f$ $\forall f \in \mathcal{F}$ have higher distortion impact and smaller delay deadline than packet k_f.

[1]The assumption of constant frame size within the same frame type in one time slot is made for clarity of presentation. However, the proposed energy management sub-system is not limited by this assumption and the extension to a general case is straightforward.

[2]It should be noted that the developed framework is also applicable in the case when the packets within one frame type have different distortion impact values.

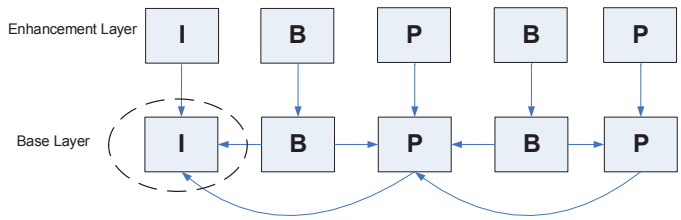

Fig. 1: GoP structure with frame dependencies [14]. For instance, the circled I frame is an ancestor for the first B and P frames in the base layer and the I frame in the enhancement layer.

B. Video Call-level Traffic Model

Video call arrivals are modeled as a Poisson process, which is a widely adopted assumption [3], [4]. In particular, the arrival process of both new and handoff video calls is modeled by a Poisson process with arrival rate λ. According to statistics, the video call duration is very likely to be heavy-tailed, which implies that most video calls have a quite short duration while a small fraction of video calls have an extremely large duration [3], [4]. For effective and tractable analysis, it is proposed in [27] to fit a large class of heavy-tailed distributions with hyper-exponential distributions. For tractability, a two-stage hyper-exponential distribution is used to model the video call duration. Hence, the probability density function (PDF) of the call duration, T_c, with mean $\bar{T}_c$, is given by [3], [4]

$$f_{T_c}(t) = \frac{a}{a+1} \cdot \frac{a}{\bar{T}_c} \cdot e^{-\frac{a}{\bar{T}_c}t} + \frac{1}{a+1} \cdot \frac{1}{a\bar{T}_c} \cdot e^{-\frac{1}{a\bar{T}_c}t}, \quad a \geq 1, t \geq 0. \tag{1}$$

User residence time, T_r, is used to characterize the user mobility within the service area, which is assumed to follow an exponential distribution, with mean $\bar{T}_r$. The channel holding time in the service area is given by $T_h = \min(T_c, T_r)$, where T_c and T_r are independent of each other. As a result, the PDF of the channel holding time is given by

$$f_{T_h}(t) = \frac{a}{a+1} \cdot (\frac{1}{\bar{T}_r} + \frac{a}{\bar{T}_c}) \cdot e^{-(\frac{1}{\bar{T}_r} + \frac{a}{\bar{T}_c})t} + \frac{1}{a+1} \cdot (\frac{1}{\bar{T}_r} + \frac{1}{a\bar{T}_c}) \cdot e^{-(\frac{1}{\bar{T}_r} + \frac{1}{a\bar{T}_c})t}, \quad t \geq 0. \tag{2}$$

C. Video Transmission Model

Consider an uplink live video transmission from an MT [5]. The MT is equipped with multiple radio interfaces and has multi-homing capabilities. As a result, the MT can establish communications with multiple wireless networks simultaneously and employ them for video packet transmission. Let $\mathcal{N} = \{1, 2, \ldots, N\}$ denote the utilized radio interfaces, and $N \geq 2$.

The uplink bandwidth allocated to the MT for radio interface n is denoted by b_n, which can be determined using a resource allocation mechanism similar to that in [2] - [4]. The offered bandwidth to the MT varies according to call arrivals and departures. Since call arrivals follow a Poisson process, the channel holding time follows a general distribution, and all calls are served without queueing, an $M/G/\infty$ model can be used to capture the statistics of number of calls that are simultaneously in service [3], [4][3]. Hence, using the statistics of number of calls in service and the resource allocation mechanism, the probability that bandwidths $b_1, b_2, \ldots, b_N$ are offered to radio interfaces $1, 2, \ldots, N$, $f_{B_1,B_2,\ldots,B_N}(b_1, b_2, \ldots, b_N)$, can be derived based on a Poisson distribution with mean $\upsilon = \lambda \cdot E[T_h]$ [3], [4], where $E[T_h]$ is the average channel holding time which can be calculated from (2).

The average transmission power allocated to radio interface n is denoted by $\bar{P}_n$. Let γ_n denote the received signal-to-noise ratio (SNR) at the base station (BS) or access point (AP) communicating with radio interface n. It is assumed that the channel conditions do not change much during one time slot, hence the received SNR value, γ_n, $\forall n \in \mathcal{N}$, is constant within one time slot and varies independently from one time slot to another [5], [11], [12]. This model fits a pedestrian mobile user whose distance from the serving BSs/APs does not change significantly during the call.

Each radio interface, $n \in \mathcal{N}$, can support a discrete set of data rates r_{n,m_n}, with $m_n \in \mathcal{M} = \{1, 2, \ldots, M\}$. Radio interface $n \in \mathcal{N}$ can support data rate r_{n,m_n} if the received SNR value, γ_n, for this radio interface exceeds some threshold Γ_{n,m_n}. The set of thresholds Γ_{n,m_n}, $\forall n \in \mathcal{N}, m_n \in \mathcal{M}$, can be calculated using Shannon formula as

$$\Gamma_{n,m_n} = 2^{\frac{r_{n,m_n}}{b_n}} - 1, \quad n \in \mathcal{N}, m_n \in \mathcal{M} \tag{3}$$

and $\Gamma_{n,M+1}$ is assumed to be ∞.

For each time slot, let x_{kn}^f denote a video packet scheduling decision, where $x_{kn}^f = 1$ if packet k of frame f is assigned to radio interface n, otherwise $x_{kn}^f = 0$, and P_n is the instantaneous transmission power allocation to radio interface n. The circuit power required to keep radio interface n active is denoted by P_{cn} [4]. The MT available energy at the beginning of the call is denoted by E.

IV. Energy Management Sub-system Design

In this section, an MT energy management sub-system is presented for sustainable multi-homing video transmission over a target call duration. The energy management sub-system consists of two stages. The first stage takes place during call set-up and aims to determine an optimal QoS lower bound

[3]A more accurate system model that accounts for call blocking probability follows an $M/G/K/K$ queue. However, an exact solution for the $M/G/K/K$ model is only possible for special cases, such as for exponential service and/or a single server, and approximation models are used [28]. In this paper, to simplify the analysis, we approximate the system model as an $M/G/\infty$ queue, which significantly reduces computational complexity, as the statistics eventually follows Poisson distribution.

[4]For a data call, both the call duration and hence power consumption are affected by the transmission data rate, for a given file size. Conventionally, data transmission using lowest modulation order would reduce transmission power, which however also leads to a longer call duration. As a result, circuit power consumption for data calls makes the lowest modulation order transmission a poor strategy for energy saving. Different from that, in video streaming, the call duration is not affected by the transmission data rate. Hence, the only effect of including the circuit power consumption is that, instead of supporting a target video quality q_1, we might only be able to support a lower quality value $q_2 (< q_1)$.

that can be supported over the call duration, given the MT available energy, target call duration, and video and radio interface characteristics, which is discussed in Section IV.A. The second stage takes place during the call where the MT adapts its energy consumption to satisfy at least the target video quality lower bound calculated in the call set-up, which is discussed in Section IV.B. It is assumed that the energy consumed in the computation of the energy management subsystem is negligible as compared to the transmission energy consumption [10]. Two benchmarks are also discussed for comparison.

A. Statistical QoS Guarantee for Wireless Multi-homing Video Transmission

In the call set-up stage, the main objective is to find the maximum QoS lower bound that can be supported with statistical guarantee for multi-homing video transmission.

Let Q_t denote the video quality metric which is defined as the distortion impact ratio of the transmitted packets to the total available packets in time slot t. Due to channel fading and time varying offered bandwidth (and hence time varying data rates at different radio interfaces) and packet encoding statistics, the video quality metric Q_t is a discrete random variable. For a stationary and ergodic process of system dynamics (in terms of channel fading, offered bandwidth, and packet encoding), the time subscript t of Q_t can be omitted. Hence, Q is given as

$$Q = \frac{\sum_{k_f, f\in\mathcal{F}} \sum_{n\in\mathcal{N}} x_{kn}^f v_f}{\sum_{k_f, f\in\mathcal{F}} v_f}. \quad (4)$$

We aim to find the video quality CDF, $F_Q(q)$, given the MT available energy, the time varying offered bandwidth and channel conditions at different radio interfaces, the target call duration, and the video packet characteristics in terms of distortion impact, delay deadlines, and packet encoding statistics. Using the video quality CDF, we can find the video quality lower bound, q_l, that can be supported by the MT for the target call duration such that $\Pr(Q \le q_l) \le \epsilon_q$, with $\epsilon_q \in [0,1]$. This is achieved following a three-step framework: 1) The probability of employing a given set of data rates at different radio interfaces is calculated; 2) Using a video packet scheduling algorithm, given the frame size and data rate statistics, we find the video quality PMF and hence calculate the video quality CDF; and 3) Through optimal average power allocation to different radio interfaces, we find the maximum video quality lower bound, q_l, that can be supported for the target call duration. This is discussed in more details in the following.

1) Data Rate PMF: In a fading channel, the received SNR value, γ_n, at radio interface $n \in \mathcal{N}$, is larger than a threshold, Γ_{n,m_n}, given $B_n = b_n$, with conditional probability[5]

$$p_{n,m_n|b_n} = \Pr(\gamma_n > \Gamma_{n,m_n} | B_n = b_n). \quad (5)$$

[5]Since we perform power allocation, the offered bandwidth affects the transmission power and hence the received SNR γ_n.

The probability that data rate r_{n,m_n} is used at radio interface n, $m_n \in \mathcal{M}$, is given by

$$\psi_{n,m_n|b_n} = p_{n,m_n|b_n} - p_{n,m_n+1|b_n}, \qquad m_n \in \mathcal{M}. \quad (6)$$

For independent fading statistics at different radio interfaces, the conditional probability that data rates $r_{1,m_1}, r_{2,m_2}, \ldots, r_{N,m_N}$ are used at radio interfaces $1, 2, \ldots, N$ can be calculated as

$$f_{R_{1,m_1},\cdots,R_{N,m_N}|B_1,\cdots,B_N}(r_{1,m_1},\cdots,r_{N,m_N}|b_1,\cdots, b_N) = \prod_{n=1}^{N} \psi_{n,m_n|b_n}. \quad (7)$$

Let $\mathcal{B}$ denote the set of offered bandwidths to the MT. The probability that data rates $r_{1,m_1}, r_{2,m_2}, \ldots, r_{N,m_N}$ are used at radio interfaces $1, 2, \ldots, N$ can be calculated as

$$f_{R_{1,m_1},\cdots,R_{N,m_N}}(r_{1,m_1},\cdots,r_{N,m_N}) = \sum_{\mathcal{B}} f_{R_{1,m_1},\cdots,R_{N,m_N}|B_1,\cdots,B_N}(r_{1,m_1},\cdots,r_{N,m_N}|b_1, \cdots, b_N) \cdot f_{B_1,\ldots,B_N}(b_1,\ldots,b_N). \quad (8)$$

For instance, in a Rayleigh fading channel, γ_n follows an exponential distribution, which is given by

$$f_{\Upsilon_n}(\gamma_n) = \frac{1}{\bar{\gamma}_n} \cdot e^{-\frac{\gamma_n}{\bar{\gamma}_n}}, \qquad n \in \mathcal{N} \quad (9)$$

where $\bar{\gamma}_n = \frac{\bar{P}_n \Omega_n}{b_n \eta_0}$ denotes the average received SNR for radio interface n, Ω_n denotes the average channel power gain for radio interface n, and η_0 denotes the one-sided noise power spectral density. Hence, $f_{R_{1,m_1},\cdots,R_{N,m_N}}(r_{1,m_1},\cdots,r_{N,m_N})$ is given by

$$f_{R_{1,m_1},\cdots,R_{N,m_N}}(r_{1,m_1},\cdots,r_{N,m_N}) = \sum_{\mathcal{B}} \prod_{n=1}^{N} (e^{-\frac{\Gamma_{n,m_n}}{\bar{\gamma}_n}} - e^{-\frac{\Gamma_{n,m_n+1}}{\bar{\gamma}_n}}) \cdot f_{B_1,\ldots,B_N}(b_1,\ldots,b_N). \quad (10)$$

2) Video Quality CDF: In the following, we aim to find the video quality q that can be achieved given the MT data rates r_{n,m_n} at different radio interfaces and frame size c_f with f belongs to I, P, and B types. Using the data rate and packet encoding statistics, we find the video quality CDF, $F_Q(q)$.

Since video packets that belong to the same frame have the same delay deadline of the frame, the required rate to transmit a packet k_f, $\forall f \in \mathcal{F}$, is given by $r(k_f) = l_f/\Delta D_{f+1,f}$ [5]. The scheduled packets to a given radio interface, n, should satisfy

$$\sum_{k_f, f\in\mathcal{F}} x_{kn}^f r(k_f) \le r_{n,m_n}, \qquad \forall n \in \mathcal{N}, m_n \in \mathcal{M}. \quad (11)$$

Video packet scheduling should capture the dependence relationship among different video packets within the same time slot. Packets which ancestors are not scheduled for transmission should not be transmitted since they will not be successfully decoded at the destination and thus waste the MT and network resources. This requirement can be expressed by a precedence constraint given by

$$x_{kn}^f \le x_{k'n'}^{f'}, \qquad \forall k'_{f'} \in \mathcal{A}_k^f, n, n' \in \mathcal{N}. \quad (12)$$

Finally, a video packet should be assigned to one and only one radio interface, that is

$$\sum_{n=1}^{N} x_{kn}^{f} \leq 1, \quad \forall k_f, f \in \mathcal{F}. \tag{13}$$

Hence, multi-homing video packet scheduling, given the available data rates $r_{1,m_1}, r_{2,m_2}, \ldots, r_{N,m_N}$ at different radio interfaces and frame size c_f with f belonging to I, P, and B types, should satisfy

$$\begin{aligned} \max_{x_{kn}^{f}} \quad & q \\ s.t. \quad & (11)-(13) \\ & x_{kn}^{f} \in \{0,1\}. \end{aligned} \tag{14}$$

The optimization problem (14) is a binary program. Problem (14) can be mapped to a new variant of the knapsack problem, referred to as precedence-constrained multiple knapsack problem (PC-MKP) [22]. The available items are the video packets, $k_f \; \forall f \in \mathcal{F}$, the item weights are the required data rates, $r(k_f)$, and the profit associated with each item is the packet distortion impact value, v_f. As we have multiple radio interfaces, the problem has multiple knapsacks each with capacity r_{n,m_n}. Due to the dependencies among different video packets within the time slot, the MKP has the precedence constraint (12). Since the knapsack problems are NP-hard [29], the PC-MKP is also NP-hard. We present a greedy algorithm that can solve the PC-MKP of (14) in polynomial time based on [30]. Video packets are first classified into root and leaf items. In general, root items have higher precedence order than leaf items. For video packet transmission, root items (packets of I and P frames) have higher distortion impact than leaf items (packets of B frames) [11]. Let $\mathcal{L}$ denote the set of unassigned packets, u_n the current used capacity at radio interface n (the remaining capacity is $o_n = r_{n,m_n} - u_n$), $\mathcal{S}_n$ the set of assigned packets to radio interface n ($\mathcal{S} = \bigcup_{n=1}^{N} \mathcal{S}_n$), and h_{kf} an index of the radio interface where packet k_f is currently assigned to. The multi-homing video packet scheduling algorithm is described in Algorithm 1.

Algorithm 1 has two parts. In the first part (A1), we aim to find a feasible solution for the problem through assigning items (video packets) with the highest profit (distortion impact) to different knapsacks (radio interfaces) while considering their precedence constraints. In the second part (A2), we aim to improve the feasible solution of A1. This is achieved by considering all pairs of packed items (video packets) and, if possible, interchanges them whenever doing so allows the insertion of an additional item (video packet) from the remaining ones, if all its ancestors are packed, into one of the knapsacks (radio interfaces). In A2 of Algorithm 1, $\mathcal{S}, \mathcal{L}, o_n$, and h_{kf} are updated whenever some $\mathcal{S}_n$ is updated. If the total number of available video packets in a given time slot is $\sum_{f\in\mathcal{F}} c_f$, then the complexity of Algorithm 1 is $O(\sum_{f\in\mathcal{F}} c_f N) + O(\{\sum_{f\in\mathcal{F}} c_f\}^2)$, i.e., has polynomial time complexity in terms of the number of radio interfaces and video packets.

Algorithm 1 Multi-homing Video Packet Scheduling

A1: Finding a Feasible Solution
Input: $r_{n,m_n} \; \forall n \in \mathcal{N}$, $c_f \; \forall f \in \mathcal{F}$;
Initialization: $\mathcal{L} \longleftarrow \bigcup_{f\in\mathcal{F}} k_f$, $u_n \longleftarrow 0$, $\mathcal{S}_n = \{\} \; \forall n \in \mathcal{N}$;
for $n \in \mathcal{N}$ **do**
  for $k_f \in \mathcal{L}$ **do**
    if $x_{k'n'}^{f'} = 1 \; \forall k'_{f'} \in \mathcal{A}_k^f, n' \in \mathcal{N}$, $r(k_f) + u_n \leq r_{n,m_n}$ **then**
      $x_{kn}^{f} = 1$, $u_n = u_n + r(k_f)$;
    end if
    $\mathcal{S}_n = \mathcal{S}_n \cup \{k_f\}$;
  end for
  $\mathcal{L} = \mathcal{L} - \mathcal{S}_n$;
end for
for $n \in \mathcal{N}$ and $o_n > \min\{r(k_f)|k_f \in \mathcal{L}\}$ **do**
  for $k_f \in \mathcal{L}$ **do**
    if $x_{k'n'}^{f'} = 1 \; \forall k'_{f'} \in \mathcal{A}_k^f, n' \in \mathcal{N}$, $r(k_f) + u_n \leq r_{n,m_n}$ **then**
      $x_{kn}^{f} = 1$, $u_n = u_n + r(k_f)$;
    end if
    $\mathcal{S}_n = \mathcal{S}_n \cup \{k_f\}$;
  end for
  $\mathcal{L} = \mathcal{L} - \mathcal{S}_n$;
end for
A2: Improving the Feasible Solution
for $k1 \in \{k_f|k_f \in \mathcal{S}, o_{h_{kf}} + \max_{n\neq h_{kf}} o_n \geq \min_{k'_{f'}\in\mathcal{L}} r(k'_{f'})\}$ **do**
  for $k2 \in \{k_f|k_f \in \mathcal{S}, k_f > k1, h_{kf} \neq h_{k1}, o_{h_{k_f}} + o_{h_{k1}} \geq \min_{k'_{f'}\in\mathcal{L}} r(k'_{f'})\}$ **do**
    $W(a) = \max\{r(k1), r(k2)\}$, $W(b) = \min\{r(k1), r(k2)\}$;
    $i_a = h_a$, $i_b = h_b$, $\delta = W(a) - W(b)$;
    if $\delta \leq o_{i_b}$ and $o_{i_a} + \delta \geq \min_{k'_{f'}\in\mathcal{L}} r(k'_{f'})$ **then**
      $v_c = \max\{v_{k'_{f'}}|k'_{f'} \in \mathcal{L}, r(k'_{f'}) \leq o_{i_a} + \delta, \mathcal{A}_{k'}^{f'} \subset \mathcal{S}\}$;
      $\mathcal{S}_{i_a} = (\mathcal{S}_{i_a} - a) \cup \{b, c\}$, $\mathcal{S}_{i_b} = (\mathcal{S}_{i_b} - b) \cup \{a\}$;
    end if
  end for
end for
Output: $q = \frac{\sum_{k_f, f\in\mathcal{F}} \sum_{n\in\mathcal{N}} x_{kn}^{f} v_f}{\sum_{k_f, f\in\mathcal{F}} v_f}$.

Using Algorithm 1, the video quality q that can be achieved using data rates $r_{1,m_1}, r_{2,m_2}, \ldots, r_{N,m_N}$ at radio interfaces $1, 2, \ldots, N$ and frame size c_f with f belonging to I, B, and P types can be calculated. The set of different data rates and packet encoding combinations that result in the same video quality q is denoted by $\mathcal{Q}$. We can map the data rate and frame size statistics into a video quality PMF given by

$$\begin{aligned} f_Q(q) = \sum_{\mathcal{Q}} \{ & f_{R_{1,m_1},\cdots,R_{N,m_N}}(r_{1,m_1}, \cdots, r_{N,m_N}) \\ & \cdot f_{C_I,C_B,C_P}(c_I, c_B, c_P)\} \end{aligned} \tag{15}$$

where $f_{C_I,C_B,C_P}(c_I, c_B, c_P)$ denotes the joint PMF of video packet encoding for I, B, and P frames which is given as the multiplication of the PMFs of I, B, and P frames assuming an

i.i.d. frame size statistics [11]. As a result, the video quality CDF, $F_Q(q)$, can be calculated.

3) Maximum QoS Lower Bound That Can Be Achieved with Statistical Guarantee: From (10), the probability that data rates r_{n,m_n} are used at different radio interfaces depends on the average received SNR values, $\bar{\gamma}_n \ \forall n \in \mathcal{N}$. As a result, the video quality CDF is a function of the average transmission power at different radio interfaces. Hence, the distribution of the average transmission power, $\frac{E}{\widetilde{T}_c}$, among different radio interfaces, i.e., $\bar{P}_n$, affects the resulting video quality CDF.

Since T_c is a random variable, we aim to guarantee that the MT available energy can support a target call duration, $\widetilde{T}_c$. Hence, we first find $\widetilde{T}_c$ that satisfies $\Pr(T_c \leq \widetilde{T}_c) \geq 1 - \epsilon_c$, $\epsilon_c \in [0, 1]$, using the call duration PDF given in (1). Assuming an ergodic process of system dynamics, in order to find the maximum video quality lower bound, q_l, that can be supported for the target call duration, $\widetilde{T}_c$, with some statistical guarantee, ϵ_q, we need to solve

$$\begin{aligned} \max_{\bar{P}_n \geq 0} \quad & q_l \\ s.t. \quad & F_Q(q_l) \leq \epsilon_q \\ & \sum_{n=1}^{N} (\bar{P}_n + P_{cn}) \leq \frac{E}{\widetilde{T}_c}. \end{aligned} \tag{16}$$

The first constraint in (16) has an inequality (instead of an equality) since the supported data rates at different radio interfaces form a discrete set, and hence the achieved video quality is also discrete. As a result, an equality in the first constraint of (16) cannot always be satisfied, unlike the inequality. In (16), ϵ_q is a design parameter that can be chosen to strike a balance between the desired performance (in terms of the video quality and energy consumption) and success probability of the call delivery. This issue is further investigated in the simulation results Section. The second constraint is for the average power consumption of the MT which is based on the total available energy and the target call duration. In the proposed energy management sub-system, the MT cannot have average energy consumption greater than that value.

Heuristic optimization techniques, e.g., the Genetic Algorithm (GA) [31], can be used to solve the optimization problem (16). The GA can be easily implemented in smart phones as it consists of simple iterations. In addition, using the GA in solving (16) is fast due to the small number of variables (the number of radio interfaces can be from 2 to 4).

Following (16), the MT can support a multi-homing video quality at least equals to q_l for the call duration, T_c, with an outage probability ϵ_s, given as

$$\begin{aligned} \epsilon_s &= 1 - \Pr(Q \geq q_l | T_c \leq \widetilde{T}_c) \cdot \Pr(T_c \leq \widetilde{T}_c) \\ &= 1 - (1 - \epsilon_q) \cdot (1 - \epsilon_c). \end{aligned} \tag{17}$$

B. Energy Efficient QoS Provision for Wireless Multi-homing Video Transmission

During the call, the MT adapts its energy consumption to satisfy at least the maximum video quality lower bound, q_l, calculated in the call set-up. At good channel and/or network conditions, the MT achieves video quality better than the lower bound, however, at bad conditions the MT satisfies a quality not less than the lower bound. This is performed in three steps: 1) The MT determines the total required data rate, at the current time slot, in order to satisfy at least q_l, given the current time slot video packet encoding; 2) The MT determines the minimum power required at each radio interface, and hence the required data rate at each radio interface, in order to satisfy the total required data rate calculated in 1), given the current time slot channel fading and offered bandwidth; and 3) The MT performs video packet scheduling given the data rate at each radio interface, calculated in 2). These are discussed in more details in the following.

1) Total Required Data Rate: Due to the time varying video packet encoding (i.e., c_f for f belongs to I, B, and P packets), the total required data rate in order to satisfy at least the video quality lower bound, q_l, varies over time. As a result, at the beginning of each time slot, t, given the available video packets ready for transmission, the MT determines the total required data rate, r, that satisfies at least the video quality lower bound. Let q_t denote the resulting video quality that can be achieved at time slot t by scheduling a set $\mathcal{S}$ of video packets for transmission. The total required data rate, r, can be calculated using Algorithm 2.

Algorithm 2 Calculation of Total Required Data Rate to Satisfy QoS Lower Bound

Input: $c_f \ \forall f \in \mathcal{F}$;
Initialization: $\mathcal{L} \longleftarrow \underset{f \in \mathcal{F}}{\cup} k_f$, $r \longleftarrow 0$, $\mathcal{S} = \{\}$;
while $q_t < q_l$ **do**
  if $x^f_{k'_{f'} n'} = 1 \ \forall k'_{f'} \in \mathcal{A}^f_k, n' \in \mathcal{N}$ **then**
    $x^f_{kn} = 1$, $r = r + r(k_f)$;
  end if
  $\mathcal{S} = \mathcal{S} \cup \{k_f\}$;
end while
Output: r.

In Algorithm 2, it is assumed that video packets are sorted according to their classification as root and leaf items. Algorithm 2 finds the total data rate required to satisfy at least the video quality lower bound, q_l, by scheduling video packets with the highest distortion impact for transmission until q_l at least is satisfied.

2) Minimum Power Allocation: Due to the time varying offered bandwidths and channel conditions at different radio interfaces, the required transmission power allocation, P_n, to satisfy the total data rate, r, needs to be determined at the beginning of every time slot t. Assuming available perfect channel state information (CSI) [32] and through transmission power allocation, the received SNR value, γ_n, for different radio interfaces can be determined. When γ_n exceeds threshold Γ_{n,m_n}, radio interface n can support data rate r_{n,m_n}. Hence, transmission power allocation affects the resulting data rate at each radio interface, r_{n,m_n}. As a result, the objective is to find the minimum transmission power allocation to different radio interfaces, which is required to satisfy the total data rate r calculated in Algorithm 2. Let E_t denote the MT available energy at the beginning of time slot t. The transmission power

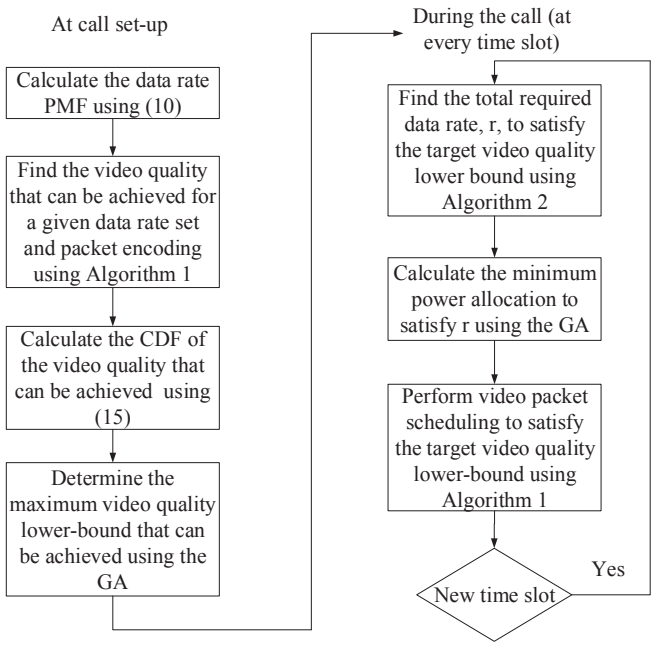

Fig. 2: Flow chart of the proposed energy management sub-system procedure.

allocation problem can be described as

$$\begin{aligned} \min_{P_n \geq 0} \quad & \sum_{n=1}^{N} (P_n + P_{cn})\tau \\ s.t. \quad & \sum_{n=1}^{N} r_{n,m_n} \geq r \\ & \sum_{n=1}^{N} (P_n + P_{cn})\tau \leq E_t. \end{aligned} \tag{18}$$

Similar to (16), (18) can be solved using the GA. Hence, every time slot with duration τ, the MT updates its transmission power allocation P_n to each radio interface n to satisfy its target video quality.

3) Video Packet Scheduling: Using the data rates, r_{n,m_n}, that can be supported through the transmission power allocation, P_n, calculated in (18), Algorithm 1 is used to schedule the current time slot available video packets for transmission. The resulting video quality satisfies the lower bound q_l, calculated in (16), over the entire call duration with a success probability ϵ_s.

The energy management sub-system procedure for supporting a sustainable video transmission over the call duration with consistent video quality is summarized in Figure 2.

C. Implementation Complexity

The proposed energy management sub-system works in two stages. The first stage can be easily implemented using a look-up table. A look-up table can be stored at the MT to derive the CDF of the video quality that can be achieved, as given in (15). Sample packet encoding PMF can be used according to the video type (high motion or low motion). In addition, the discrete set of data rates and offered bandwidths that can be used at different radio interfaces can be provided to the MT. Hence, using the packet scheduling algorithm in Algorithm 1 and given the packet encoding statistics and allowed data rates at different radio interfaces, a look-up table can be created with two columns, the first column gives the video quality that can be achieved and the second column gives the corresponding probability as a function of the the average received SNR values, $\bar{\gamma}_n$ $\forall n$, and the offered bandwidth statistics. Once $\bar{\gamma}_n$ $\forall n$ and the offered bandwidth statistics are specified online, an approximate expression of the achievable CDF of the video quality is obtained. The GA is then used to determine the maximum QoS lower bound that can be achieved, which can be simply implemented since we have a small number of decision variables (average power allocation at MT radio interfaces, e.g., 2 to 3 radios). The second stage, which takes place during the call, has three parts. The first part is implemented using a simple while loop, as in Algorithm 2, that keeps adding packets until a minimum quality is satisfied. The second part is based on GA which again is simple to implement due to a small number of decision variables. The last part, which is implemented using Algorithm 1, is shown to have a polynomial time complexity.

D. Benchmarks

In this sub-section, two benchmarks are presented for comparison. The first benchmark aims to maximize the resulting video quality in the absence of an energy management sub-system, similar to [14] - [16]. The second benchmark satisfies an energy budget per time slot for energy management, similar to [13] and [22].

1) Multi-homing Video Transmission Without Energy Management: In the absence of an energy management sub-system, the main objective is to maximize the resulting video quality subject to the MT battery energy limitation. Intuitively, the higher the achieved data rates at different radio interfaces, subject to the MT battery energy limitation, the more transmitted video packets and thus the better video quality. Hence, at the beginning of every time slot t, the MT performs transmission power allocation at different radio interfaces to maximize the resulting sum data rate. This is given by

$$\begin{aligned} \max_{P_n \geq 0} \quad & \sum_{n=1}^{N} r_{n,m_n} \\ s.t. \quad & \sum_{n=1}^{N} (P_n + P_{cn})\tau \leq E_t. \end{aligned} \tag{19}$$

Problem (19) is solved using the GA. Given the transmission power allocation, P_n, and hence the data rates r_{n,m_n} $\forall n \in \mathcal{N}$, Algorithm 1 is used to schedule the current time slot available video packets for transmission.

2) Multi-homing Video Transmission With Uniform Energy Management: In this case a uniform energy budget per time slot is considered. Hence, the MT available energy at time slot t is uniformly distributed over the remaining time slots. The energy budget per time slot, starting from time slot t, is given by $E_{bt} = \frac{E_t}{T-t}$. Since T is a random variable, the average

call duration $\bar{T}_c$ is used instead of T. At the beginning of time slot t, the MT determines the maximum data rate that can be supported at each radio interface through transmission power allocation subject to the energy budget constraint. This is achieved by solving (19) while replacing E_t in the problem constraint by E_{bt}. Given the resulting data rates r_{n,m_n} $\forall n \in \mathcal{N}$, Algorithm 1 is used to schedule the available video packets for transmission in the current time slot.

V. Simulation Results and Discussion

This section presents simulation results for the proposed energy management sub-system. Video sequences are compressed at an encoding rate of 30 fps [14]. The GoP structure consists of 13 frames with one layer (base layer) and one B frame between P frames. As a result, the time slot duration τ is 433 milli-seconds. In practice, the PMFs of the I, B, and P frame sizes can be generated using the video trace as in [25]. For simplicity, sample PMFs of the I, B, and P frame sizes are arbitrary generated as shown in Figure 3. The decoder time stamp difference between two successive frames, ΔD, is 40 milli-seconds [5]. Each video packet requires a transmission data rate of 2 Kbps. The video packet distortion impact values are $v_f = 5$ for I frames, $v_f = 4$ for P frames, and $v_f = 2$ for B frames [14]. Two radio interfaces are used for video transmission ($N = 2$). The circuit power for each radio interface is 10 mW. The call arrival rate to service area $\lambda = 0.5$ call/minute and the average call duration $\bar{T}_c = 20$ minutes. Hence, the offered bandwidth statistics on the two radio interfaces can be described as

$$B = 500 \begin{bmatrix} 2 & 1 & 0.75 & 0.5 & 0.25 \\ 3 & 2 & 1.5 & 1 & 0.5 \end{bmatrix}$$

$$f_{B_1,B_2}(b_1, b_2) = \begin{bmatrix} 0.2374 & 0.2409 & 0.2218 & 0.1532 & 0.1466 \end{bmatrix}$$

where the first and second rows in B denote the offered bandwidths, in KHz, on the first and second radio interfaces, respectively, and $f_{B_1,B_2}(b_1, b_2)$ denotes the probability that the bandwidths are offered to the MT and every entry in $f_{B_1,B_2}(b_1, b_2)$ corresponds to a column in B. The set of data rates that can be supported on each radio interface is $\mathcal{R} = \{0, 0.256, 0.512, 1, 1.5, 2, 2.5\}$ Mbps. Using (3), $\mathcal{R}$ is supported with different thresholds at the two different radio interfaces, for different offered bandwidths. Each radio interface suffers from a Rayleigh fading channel with average channel power gain of $\Omega_1 = 0.5031$ and $\Omega_2 = 0.4852$. It should be noted that the choice of the PMF of the I, B, and P frame sizes is made in accordance with the offered bandwidth statistics and the MT available energy such that the available resources (i.e., offered bandwidth and MT energy) are not sufficient all the time to transmit all the available video packets. This allows us to investigate the impact of the proposed energy management sub-system on the resulting video quality.

A. Performance of the Proposed Energy Management Sub-system

In the following, the performance of the proposed energy management sub-system is investigated versus MT available energy E, ϵ_q, and ϵ_c. Different performance trade-offs are demonstrated.

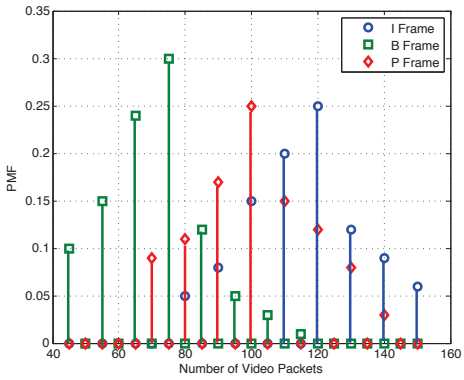

Fig. 3: The probability mass function (PMF) of I, B, and P frame sizes.

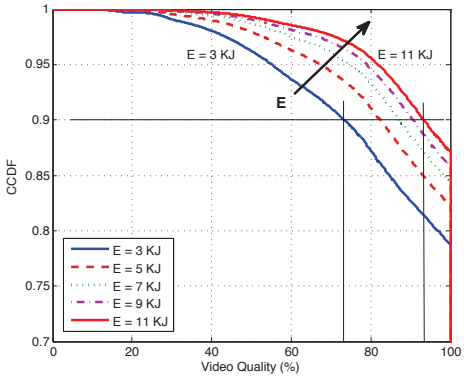

Fig. 4: The complementary cumulative distribution function (CCDF) of the achieved video quality (q) for different values of MT available energy. $\epsilon_q = 0.1$, $\epsilon_c = 0.15$, and $\bar{T}_c = 20$ minutes. The arrow shows the direction of increase of E.

Figure 7 shows the complementary cumulative distribution function (CCDF), $\Pr(Q > q)$, of the video quality (q) for $E \in [3, 11]$ KJ, $\bar{T}_c = 20$ minutes, $\epsilon_q = 0.1$, and $\epsilon_c = 0.15$. The more the available energy at the MT, the better the video quality that can be achieved with $\epsilon_q = 0.1$ and $\epsilon_c = 0.15$. For instance, with $E = 11$ KJ, a video quality of 93% can be guaranteed with probability 0.9, while a video quality of only 73% can be guaranteed with probability 0.9 for $E = 3$ KJ.

Figure 5 plots the video quality lower bound, q_l, that can be achieved with different ϵ_q values, versus the MT available energy. Higher video quality can be supported with a lower probability $(1 - \epsilon_q)$, for a given MT available energy. For instance, with $E = 4$ KJ, a video quality of 89% can be achieved with probability 0.85 (i.e., $\epsilon_q = 0.15$), while a video quality of 63% can be guaranteed with probability 0.95 (i.e., $\epsilon_q = 0.05$) at the same E.

Figure 6 plots the video quality lower bound, q_l, that can be achieved with different ϵ_c values, versus the MT available energy. The higher the statistical guarantee $1-\epsilon_c$ for the target call duration (i.e., the smaller the ϵ_c value), the larger the target call duration, and hence the lower video quality that can be supported, for a given MT available energy. For instance, with

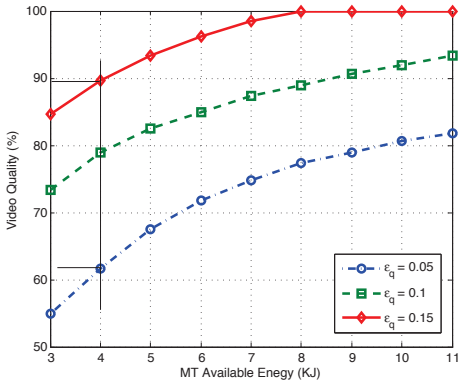

Fig. 5: The video quality lower bound that can be supported (q_l) versus MT available energy (E) for different ϵ_q. $\bar{T}_c = 20$ minutes.

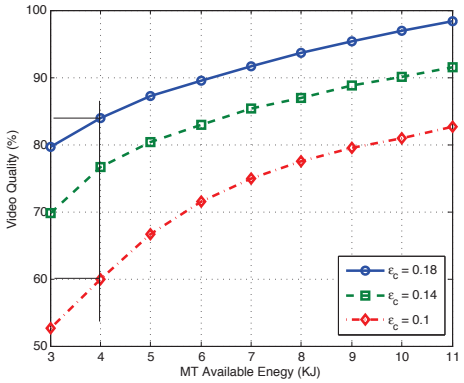

Fig. 6: The video quality lower bound that can be supported (q_l) versus MT available energy (E) for different ϵ_c. $\bar{T}_c = 20$ minutes.

$E = 4$ KJ, a video quality of 84% can be achieved with probability 0.82 (i.e., $\epsilon_c = 0.18$), while a video quality of 60% can be guaranteed with probability 0.9 (i.e., $\epsilon_c = 0.1$) at the same E.

B. Performance Comparison

In the following, the performance of the proposed energy management sub-system is compared with that of the two benchmarks in Section IV. The proposed energy management sub-system is referred to as statistical guarantee framework (SGF), while the first benchmark is referred to as total energy framework (TEF), and the second benchmark is referred to as equal energy framework (EEF). A video call is established using the three frameworks. The available energy at the beginning of the call for the three frameworks is 3 KJ. For the SGF, the video quality lower bound, q_l, is calculated in the call set-up, and equals to 89%, with $\epsilon_q = 0.1$ and $\epsilon_c = 0.3$.

Figure 7 plots the achieved video quality over the call duration using EEF, SGF, and TEF. The TEF uses up all the MT available energy and hence drain its battery before call completion. This is because the TEF main objective is to maximize the video quality in the current time slot, without considering the impact of the consumed energy on the video quality in the remaining time slots. The EEF takes into consideration the target call duration by equally distributing the MT available energy over the remaining time

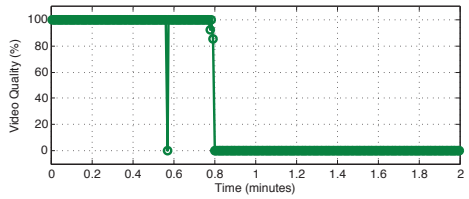

(a) Total energy framework.

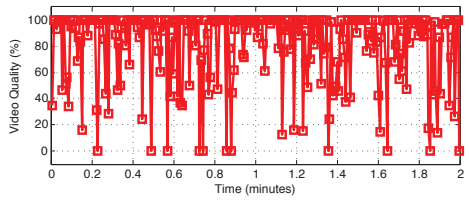

(b) Equal energy framework.

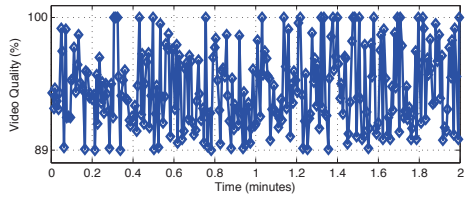

(c) Proposed statistical guarantee framework.

Fig. 7: Performance comparison for the achieved video quality versus time using TEF, EEF, and SGF. $E = 3$ KJ, $\epsilon_q = 0.1$, and $\epsilon_c = 0.3$.

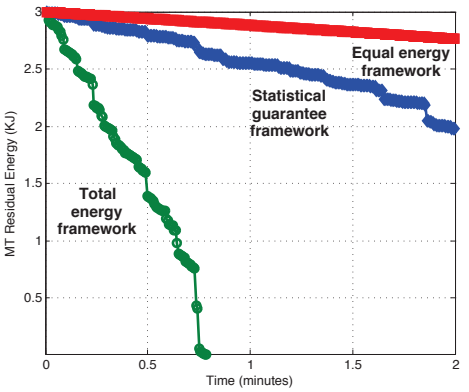

Fig. 8: The MT residual energy versus time. $E = 3$ KJ, $\epsilon_q = 0.1$, and $\epsilon_c = 0.3$.

slots. However, due to the time-varying video packet encoding, offered bandwidths, and channel conditions at the different radio interfaces, using this uniform energy budgets leads to inconsistent temporal fluctuations in the video quality. The resulting video quality for some time slots can be 0% as shown in the figure. On the other hand, the SGF can adapt the MT consumed energy at every time slot according to the packet encoding, offered bandwidth, and channel conditions at the two radio interfaces. As a result, the SGF can support a consistent video quality over different time slots, which is at least equals to the target lower bound (89%).

Figure 8 plots the MT residual energy over the call duration. The MT residual energy using the TEF near the middle of the call is insufficient to support video transmission. Since the EEF

uses a uniform energy budget for different time slots regardless of the channel fading, the slope of the consumed energy is almost constant over the first two thirds of the call period. For the SGF, the MT consumed energy does not have an equal slope as the MT adapts its energy consumption based on video packet encoding and channel conditions at the different radio interfaces over the time slot.

The advantages of the SGF over the two benchmarks can be summarized as follows: 1) The SGF guarantees a sustainable multi-homing video transmission over the target call duration, unlike the TEF; and 2) The SGF supports a consistent video quality over different time slots through adapting its energy consumption according to the video packet encoding and channel conditions at different radio interfaces, and as a result, the SGF can control the QoS lower bound violation probability.

VI. Conclusion

In this paper, an energy management sub-system is proposed to support a sustainable multi-homing video transmission, over the call duration, in a heterogeneous wireless access medium. The proposed framework aims to satisfy a target video quality lower bound that is calculated in the call set-up, given the MT available energy at the beginning of the call, the time varying bandwidth availability and channel conditions at different radio interfaces, the target call duration, and the video packet characteristics in terms of distortion impact, delay deadlines, and video packet encoding statistics. Hence, the proposed framework enables the MT to support a consistent video quality over the call duration with a certain outage probability ϵ_s, via adapting its energy consumption according to the video packet encoding, offered bandwidth, and channel conditions at different radio interfaces. Using ϵ_s as a design parameter, the MT can strike a balance between the desired performance (in terms of the video quality and energy consumption) and success probability of the call delivery.

References

[1] M. Ismail and W. Zhuang, "Statistical QoS guarantee for wireless multi-homing video transmission," *IEEE Globecom'13*, to appear.

[2] M. Ismail and W. Zhuang, "A distributed multi-service resource allocation algorithm in heterogeneous wireless access medium," *IEEE J. Select. Areas Communications*, vol. 30, no. 2, pp. 425-432, Feb. 2012.

[3] M. Ismail, A. Abdrabou, and W. Zhuang, "Cooperative decentralized resource allocation in heterogeneous wireless access medium," *IEEE Trans. Wireless Communications*, vol. 12, no. 2, pp. 714 - 724, Feb. 2013.

[4] M. Ismail and W. Zhuang, "Decentralized radio resource allocation for single-network and multi-homing services in cooperative heterogeneous wireless access medium," *IEEE Trans. Wireless Communications*, vol. 11, no. 11, pp. 4085 - 4095, Nov. 2012.

[5] K. Pandit, A. Ghosh, D. Ghosal, and M. Chiang, "Content-aware optimization for video delivery over WCDMA," *EURASIP J. Wireless Commun. and Networking*, July 2012.

[6] L. Golubchik, J. C. S. Lui, T. F. Tung, A. L. H. Chow, W. J. Lee, G. Franceschinis and C. Anglano, "Multi-path continuous media streaming: what are the benefits?" *Performance Evaluation*, vol. 49, no. 1, pp. 429-449, Sept. 2002.

[7] M. D. Trott, "Path diversity for enhanced media streaming," *IEEE Commun. Magazine*, vol. 42, no. 8, pp. 80-87, Aug. 2004.

[8] G. Miao, N. Himayat, Y. Li, and A. Swami, "Cross-Layer optimization for energy-efficient wireless communications: a survey," *Wiley J. Wireless Commun. and Mobile Computing*, vol. 9, pp. 529-542, March 2009.

[9] G. P. Perrucci , F. H.P. Fitzek, and J. Widmer, "Survey on energy consumption entities on the smartphone platform," *Proc. IEEE VTC 2011*, pp. 1-6, May 2011.

[10] E. Rantalai, A. Karppanen, S. Granlund, and P. Sarolahti, "Modeling energy efficiency in wireless internet communication," *Proc. MobiHeld '09. ACM*, pp. 67-72, Aug. 2009.

[11] F. Fu and M. van der Schaar, "Structural solutions for dynamic scheduling in wireless multimedia transmission," *IEEE Trans. Circuits and Systems for Video Technology*, vol. 22, no. 5, pp. 727-739, May 2012.

[12] Y. Zhang, F. Fu, and M. van der Schaar, "On-Line Learning and Optimization for Wireless Video Transmission," *IEEE Trans. Signal Process.*, vol. 58, no. 6, pp. 3108-3124, June 2010.

[13] S. P. Chuah, Z. Chen, and Y. P. Tan, "Energy-efficient resource allocation and scheduling for multi-cast of scalable video over wireless networks," *IEEE Trans. Multimedia*, vol. 14, no. 4, pp. 1324-1336, April 2012.

[14] D. Jurca and P. Frossard, "Video packet selection and scheduling for multipath streaming," *IEEE Trans. Multimedia*, vol. 9, no. 3, pp. 629-641, April 2007.

[15] B. Rong, Y. Qian, K. Lu, R. Q. Hu, and M. Kadoch, "Multipath routing over wireless mesh networks for multiple description video transmission," *IEEE J. Select. Areas Communications*, vol. 28, no. 3, pp. 321-331, April 2010.

[16] X. Tong, Y. Andreopoulos, M. van der Schaar, "Distortion-driven video streaming over multihop wireless networks with path diversity," *IEEE Trans. Mobile Computing*, vol. 6, no. 12, pp. 1343-1356, Dec. 2007.

[17] W. Wang and S. Shin, "A new green-scheduling approach to maximize wireless multimedia networking lifetime via packet and path diversity," *Relaible and Autonomous Computational Science*, Part 2, pp. 167-180, 2010.

[18] I. Politis, M. Tsagkaropoulos, T. Dagiuklas, and S. Kotsopoulos, "Power efficient video multipath transmission over wireless sensor networks," *Mobile Netw Appl*, vol. 13, pp. 274-284, 2008.

[19] W. Song and W. Zhuang, "Performance analysis of probabilistic multipath transmission over video streaming traffic over multi-radio wireless devices," *IEEE Trans. Wireless Commun.*, vol. 11, no. 4, pp. 1554-1564, 2012.

[20] K. Habak, K. A. Harras and M. Youssef, "OPERETTA: an optimal energy efficient bandwidth aggregation system," *Proc. IEEE SECON*, pp. 121-129, June 2012.

[21] D. H. Bui, K. Lee, S. Oh, I. Shin, H. Shin, H. Woo, and D. Ban, "GreenBag: energy-efficient bandwidth aggregation for real-time streaming in heterogeneous mobile wireless networks," *Proc. IEEE RTSS*, Dec. 2013.

[22] M. Ismail, W. Zhuang, and S. Elhedhli, "Energy and content aware multi-homing video transmission in heterogeneous networks," *IEEE Trans. Wireless Communications*, vol. 12, no. 7, pp. 3600-3610, July 2013.

[23] Q. Du and X. Zhang, "Statistical QoS provisionings for wireless unicast/multicast of multi-layer video streams," *IEEE J. Select. Areas Communications*, vol. 28, no. 3, pp. 420-433, April 2010.

[24] J. Chakareski, S. Han, and B. Girod, "Layered coding vs. multiple description for video streaming over multiple paths," *Proc. eleventh ACM Intl. Conf. on Multimedia*, pp. 422-431, 2003.

[25] D. Fiems, B. Steyaert, and H. Bruneel, "A genetic approach to Markovian characterisation of H.264 scalable video," *Multimedia Tools Appl.*, vol. 58, no. 1, pp. 125-146, 2012.

[26] M. van der Schaar and D. Turaga, "Cross-layer packetization and retransmission strategies for delay-sensitive wireless multimedia transmission," *IEEE Trans. Multimedia*, vol. 9, no. 1, pp. 185-197, Jan. 2007.

[27] A. Feldmann and W. Whitt, "Fitting mixtures of exponentials to long-tail distributions to analyze network performance models," *Performance Evaluation*, vol. 31, no. 3-4, pp. 245-279, Jan. 1998.

[28] J. M. Smith, "M/G/c/K blocking probability models and system performance," *Performance Evaluation*, vol. 52, no. 4, pp. 237-267, 2003.

[29] H. Kellerer, U. Pferschy, and D. Pisinger, *Knapsack problems*, Springer, 2004.

[30] S. Martello and P. Toth, "Heuristic algorithms for the multiple knapsack problem," *Computing*, vol. 27, no. 2, pp. 93-112, 1981.

[31] K. F. Man, K. S. Tang, and S. Kwong, "Genetic algorithms: concepts and applications," *IEEE Trans. Industrial Electronics*, vol. 43, no. 5, pp. 519-534, Oct. 1996.

[32] D. W. K. Ng and R. Schober, "Resource allocation and scheduling in multi-cell OFDMA systems with decode-and-forward relaying," *IEEE Trans. Wireless Communications*, vol. 10, no. 7, pp. 2246-2258, July 2011.